Geomechanics and Engineering, *Vol. 41, No. 2 (2025) 275-285*
https://doi.org/10.12989/gae.2025.41.2.275

Inter-particle bonding mechanisms in biopolymer-hydrogel stabilized granular soils: A microscopic perspective

Sojeong Lee[1a] and Ilhan Chang*[2]

[1]*Korea Standard Construction Center, Korea Institute of Civil engineering and Building Technology, Goyang 10223, Korea*
[2]*Department of Civil Systems Engineering, Ajou University, Suwon, 16499, Korea*

(*Received December 8, 2024, Revised April 1, 2025, Accepted April 2, 2025*)

Abstract. Biopolymer-based soil treatment (BPST) enhances soil strength through biofilm matrix formation within soil voids. This study investigates the effects of biopolymer concentration, porosity, and soil packing conditions on biopolymer distribution and connectivity after dehydration. Laboratory experiments assessed the degree of biopolymer filling (DoBF), final condensed biopolymer concentration, and biopolymer film connectivity under simple cubic and rhombohedral packing conditions. The results show that higher initial biopolymer concentrations increase final biopolymer volume, though not proportionally due to threshold effects. Rhombohedral packing results in higher final condensed biopolymer concentrations than simple cubic packing, despite having lower DoBF values, while biopolymer connectivity peaks at an optimal porosity ($n \approx 0.35$). Further analysis revealed a strong correlation between biopolymer matrix formation and soil mechanical properties, including uniaxial compressive strength (UCS), cohesion, and friction angle. UCS was found to decrease with increasing porosity, and a predictive model was developed using experimental data. The rhombohedral and simple cubic packing conditions respectively define the upper and lower bounds of the shear parameters. A back-calculation approach confirmed that DoBF provides the most accurate estimation of friction angle and UCS, reinforcing its importance as a key parameter in soil stabilization. These findings emphasize the need for optimized biopolymer concentration and soil structure adjustments to enhance reinforcement efficiency. The study offers valuable guidance for geotechnical applications, enabling the development of optimized biopolymer injection strategies that enhance mechanical performance and promote efficient material utilization.

Keywords: biopolymer; biopolymer-based soil treatment (BPST); geotechnical engineering; Xanthan gum

1. Introduction

Ground improvement encompasses techniques aimed at enhancing the performance of foundation soils or earth structures to address critical geotechnical challenges (Schaefer *et al.* 2012). The primary goals of ground improvement include increasing soil strength, reducing erodibility, limiting deformation under applied loads, minimizing compressibility, and controlling swelling, shrinkage, and permeability (Eslami *et al.* 2019). Ground improvement techniques can be categorized into several types based on the method and materials employed: soil improvement without admixtures (e.g., dynamic compaction, vacuum preloading), soil improvement with admixtures (e.g., microbial methods, sand compaction piles), soil improvement using grouting-type mixtures (e.g., chemical stabilization, deep mixing, jet grouting), and earth reinforcement techniques (e.g., ground anchors, vegetation-based methods) (Chu *et al.* 2009).

Chemical additives are injected into soil pores to enhance soil strength during soil improvement processes involving admixtures (Makusa 2013). Conventionally, cement, lime, fly ash, and hydrophilic gels have been commonly employed in ground improvement applications. Among these, cement has been most widely used since the 1960s; however, its practical application has diminished due to adverse environmental impacts, including increased groundwater alkalinity and significant carbon dioxide gas emissions. Notably, cement used in geotechnical engineering is estimated to account for 1–2% of global carbon dioxide emissions (Chang *et al.* 2016). As environmental concerns grow, the reluctance to utilize such conventional additives have spurred a rising demand for sustainable alternatives. This shift has intensified the need for environmentally friendly construction materials, prompting extensive research into the development of novel sustainable binders (Acharya *et al.* 2017, Aparna and Bindu 2023, Orts *et al.* 2007, Saxena *et al.* 2024).

In recent years, microbial biopolymers have gained attention as a promising alternative in geotechnical engineering due to their favorable engineering properties and environmental advantages (Ayeldeen *et al.* 2016; Cabalar *et al.* 2017, Ham *et al.* 2018, Hataf *et al.* 2018, Kwon *et al.* 2023a, Latifi *et al.* 2016, Lee *et al.* 2023, Zulfikar *et al.* 2022). A key benefit of biopolymer-based soil treatment (BPST) for ground improvement is their potential to reduce greenhouse gas emissions, which is particularly significant considering that the production of one tone of cement results in nearly 0.9 tons of carbon

*Corresponding author, Associate Professor
E-mail: ilhanchang@ajou.ac.kr
[a]Ph.D., Post-Doctoral Researcher

ISSN: 2005-307X (Print), 2092-6219 (Online)

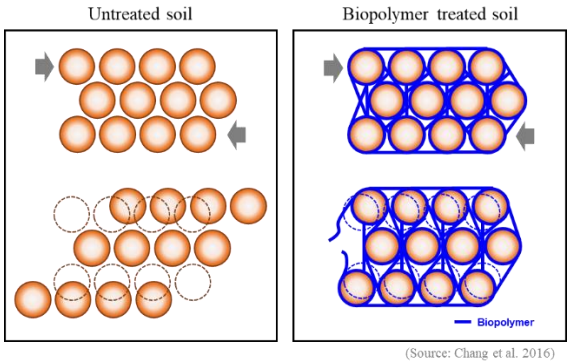

Fig. 1 Effect of biopolymer film formation under external shear force (Chang *et al*. 2016)

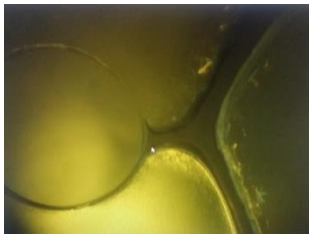

Fig. 2 Example of biopolymer film matrix formation

dioxide emissions (Barcelo *et al.* 2014). Previous studies have largely focused on evaluating the performance of microbial biopolymer treatments through laboratory tests, assessing parameters such as compressive strength, shear strength, permeability, and erosion resistance (Fatehi *et al.* 2021, Kwon *et al.* 2020, Lee *et al.* 2019a, Tran *et al.* 2019). These studies have highlighted the compatibility of microbial biopolymers as alternatives to conventional soil binders through experimental investigations, with the bonding interaction between soil particles illustrated in schematic diagrams (Fig. 1). However, a quantitative understanding of the soil bonding effect remains still underexplored. From the preliminary experimental study by authors, the bonding (bridging) effect between soil particles was verified as described in Fig. 2.

In this study, pilot study was preceded to investigate the influencing factors on the bonding effect of microbial biopolymer. The main experimental study aims to exam the impact of porosity and soil packing conditions on microbial biopolymer treatment under steady-state conditions. The prefabricated microfluidic chips were designed and utilized to replicate coarse-grained soil conditions in both pilot study and the main experimental study.

2. Materials and methods

2.1 Materials

2.1.1 Xanthan gum (XG)

Xanthan gum biopolymer (XG; $C_8H_{14}Cl_2N_2O_2$) is used in this study. It is a byproduct of *Xanthomonas campestris* bacteria and consists of two glucose molecules, two mannose molecules, and one glucuronic acid (García-Ochoa *et al.* 2000). XG is a hydrophilic and forms hydrogel when

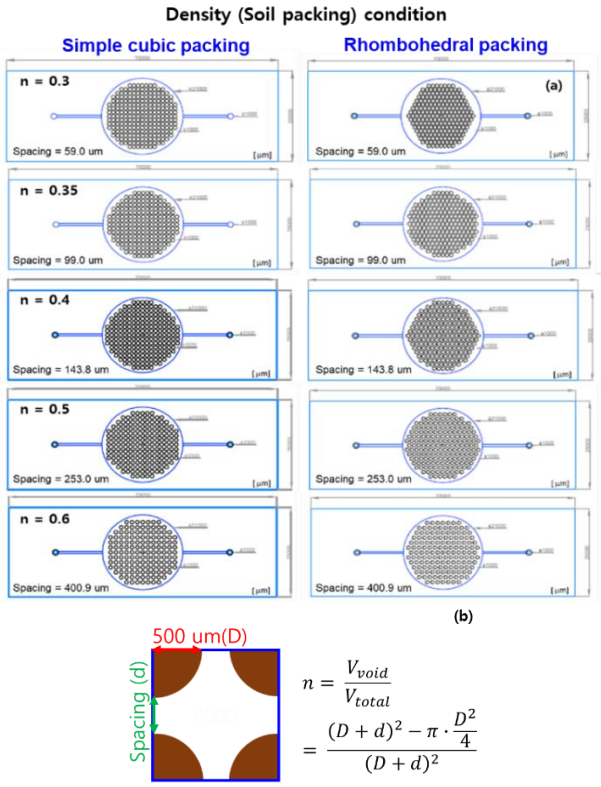

Fig. 3 Cross-sectional schematic diagram of microfluidic chips. (a) microfluidic chips with simple cubic packing conditions and rhombohedral packing; (b) porosity calculation for microfluidic chip fabrication

it absorbs water. In aqueous solutions, it forms a hydrophilic hydrogel due to negatively charged carboxyl groups (COO^-) on its side chains (Williams and Phillips, 2000). Its intermolecular interactions induce pseudoplasticity, such as shear thinning. Due to its pseudoplasticity, viscosity, and stability across a wide range of temperature and pH levels, XG is widely used in various industries (García-Ochoa *et al.* 2000, Katzbauer 1998). Recently, it has been explored as a soil stabilization and strengthening agent in geotechnical engineering (Chang *et al.* 2015a, Lee *et al.* 2019b, Chang *et al.* 2019). In this study, research-grade XG (Sigma–Aldrich, CAS number: 11138-66-2) was used for laboratory tests.

2.1.2 Microfluidic chip

Microfluidic chips are fabricated using PDMS (Polydimethylsiloxane) as shown in Fig. 3. In detail, each pillar represents sand particles with a diameter of 1 mm, and different porosity conditions are designed from 0.3 to 0.6 (i.e., 0.3, 0.35, 0.4, 0.5, 0.6). Since soil density has a significant influence on soil strength (Wei *et al.* 2020a, Shalchian *et al.* 2025), different porosity conditions were considered to investigate the behavior of biopolymer matrix formation under varying density levels. The detailed porosity calculation equation is illustrated in Fig. 3(b). To adjust pore size between particles, simple cubic packing condition and rhombohedral packing condition were reflected on microfluidic chips. Compared to the simple

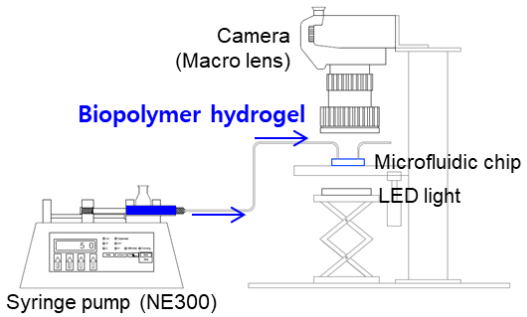

Fig. 4 Experimental set-up

cubic packing condition, the rhombohedral packing condition has a characteristic that pore space between sand particles is identical.

2.2 Methods

2.2.1 Biopolymer hydrogel preparation

The powder-form biopolymer was dissolved in deionized water using an electronic hand-mixer to achieve a homogeneous solution. The resulting solution is referred to as biopolymer hydrogel. The hydrogel concentration, expressed as a mass ratio of biopolymer to water ($m_{biopolymer}/m_{water}$) was targeted at 2.6% and 5.2%. These concentrations were determined based on the biopolymer content relative to sand ($m_{biopolymer}/m_{soil}$) at a porosity of 0.4, as outlined in Table 1. Specifically, the 2.6% and 5.2% hydrogel concentrations correspond to biopolymer contents of 1% and 2%, respectively, at the given porosity.

2.2.2 Biopolymer injected microfluidic chip preparation

The biopolymer hydrogel was injected into microfluidic chips with precision using a syringe pump (New Era Pump System NE300) at a controlled injection ratio of 50 uL/min. After the pore spaces of the microfluidic chips were completely filled, the hydrogel within the chips was allowed to dry under ambient air exposure at both the inlet and outlet.

The dehydration process was conducted over a period of 10 days under ambient conditions (≈ 22℃, 50% RH).

2.2.3 Microscopic observation

Microscopic observation was performed using a DSLR camera with a macro lens (Canon EOS R Camera; Canon MP-E 65 mm f2.8 1-5x) (Fig. 4).

3. Pilot study

3.1 Volume change of biopolymer hydrogel

Under the assumption that inter-particle bonding between biopolymer hydrogel and coarse particles are affected by soil density (porosity) and biopolymer hydrogel rheology as shown in Fig 5, different porosity and biopolymer hydrogel concentration at injection were adjusted among laboratory experiments.

Table 1 Injected biopolymer conditions (i.e., initial status)

Injecting condition		m_b/m_w*			
		2.6%		5.2%	
Porosity	V_{void} [mm^3]	m_b*	m_b/m_s*	m_b	m_b/m_s*
0.3	7.54	0.20	0.008	0.39	0.015
0.35	8.64	0.23	0.010	0.45	0.020
0..4	17.27	0.45	0.010	0.90	0.020
0.5	20.41	0.53	0.014	1.06	0.029
0.6	23.24	0.61	0.021	1.21	0.041

*m_b/m_w: $m_{biopolymer}/m_{water}$; m_b: $m_{biopolymer}$; m_b/m_s: $m_{biopolymer}/m_{soil}$

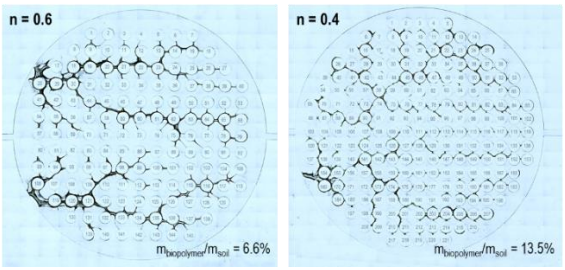

Fig. 5 Example of biopolymer film matrix formation.

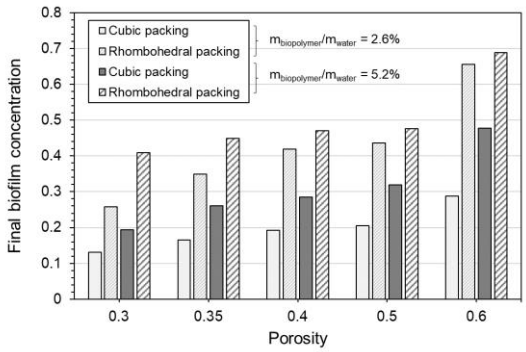

Fig. 6 Influence of porosity and packing on biofilm formation

The previous study noted that the tensile strength of XG affects behavior of biopolymer treated soils and the thresholding biopolymer concentration to cause phase change from hydrogel to film is around 20% ($m_{biopolymer}/m_{water}$) of XG (Im 2020). Thus, the final biopolymer concentration was observed additionally. Under the assumption that definite biopolymer amount was not changed in a microfluidic chip, condensed biopolymer concentration could be calculated based on final volume. Fig 6 presents a summary of the experimental findings, illustrating the relationship between porosity, soil packing conditions (i.e. simple cubic packing and rhombohedral packing), and final biofilm concentration. The results demonstrate that increasing the injected biopolymer hydrogel concentration leads to an overall increase in final biofilm concentration, irrespective of the soil porosity or packing condition. Specifically, when the biopolymer-to -water mass ratio ($m_{biopolymer}/m_{water}$) was increased from 2.6% to 5.2%, the final biofilm concentration exhibited an upward trend, though the increase was not directly proportional to the input biopolymer amount. The

rhombohedral packing condition consistently resulted in a higher final biofilm concentration compared to simple cubic packing condition under identical biopolymer hydrogel injection conditions. This suggests that the rhombohedral structure facilitates thicker biofilm development, potentially due to faster dehydration and development of tensile strength within porous matrix. Furthermore, the observation that the final biopolymer volume did not increase linearly with the doubled input concentration indicates the existence of a threshold biopolymer input beyond which additional injection does not proportionally enhance hydrogel distribution. This finding is critical for optimizing biopolymer injection strategies, suggesting that an optimal biopolymer concentration exists for maximizing hydrogel coverage while minimizing excess input.

3.2 Factors influencing final biopolymer concentration

Fig. 7 illustrates the relationship between the final biopolymer concentration and key influencing factors, including porosity, injected biopolymer hydrogel concentration, and soil packing conditions. The results indicate an increase in the final biopolymer concentration as porosity increases, aligning with the distribution trend of the final volume of dehydrated biopolymer hydrogel. Notably, the effect of pore size variations due to different soil packing conditions was almost double at the porosity level of 0.3. However, doubling the injected biopolymer hydrogel concentration did not result in a proportional doubling of the final biopolymer concentration. Additionally, the enhancement in final biopolymer concentration due to increased injected biopolymer hydrogel was more pronounced under rhombohedral soil packing conditions, particularly at lower porosity levels ranging between 0.3 and 0.4.

3.3 Expected tensile strength

Considering that XG phase changes from hydrogel to biofilm at around 20% concentration (Im 2020), effect of biopolymer hydrogel can be expected.

At porosity of 0.3, it was inferred that the phase change of injected biopolymer hydrogel occurred. Thus, brittle behavior of biofilm would be expected at failure status at porosity of 0.3. The higher injected biopolymer hydrogel concentration targeting 2% of biopolymer-soil treatment ratio ($m_{biopolymer}/m_{soil}$) would show ductile behavior at higher porosity condition than 0.35. Meanwhile, it was likely that higher tensile strength of biopolymer hydrogel works at failure when the distance between soil particles is closer and identical (i.e., rhombohedral packing condition).

4. Experimental results and analysis

4.1 Typical dehydration progress

Degree of biopolymer filling (*DoBF*), condensed biopolymer concentration ($m_{bioopolymer}/m_{w,\ final}$), and connection ratio are key parameters introduced in this study to quantify the degree of biopolymer filling within soil

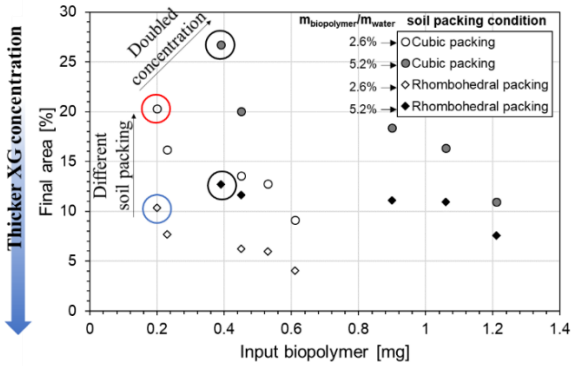

Fig. 7 Final biopolymer concentration with different porosity conditions, injected biopolymer concentrations, and soil packing conditions

voids, the concentration of biopolymer remaining after dehydration, and the extent of interconnectivity within the biopolymer network, respectively.

Degree of Biopolymer filling (DoBF) and Its Dependence on Porosity and Packing Conditions

Biopolymer dehydration over time significantly affects the final degree of biopolymer filling ($DoBF_{final}$), which is defined as the ratio of the final dehydrated/condensed biopolymer volume to the initial void volume ($V_{biopolymer\ filling}/V_{void}$). The final condensed biopolymer volume is determined based on a two-dimensional projection of the biopolymer filling.

Fig. 8(a) illustrates the variation in $DoBF_{final}$ as a function of porosity, showing that simple cubic packing condition consistently achieves a higher final degree of biopolymer filling compared to rhombohedral packing condition. Regardless of soil packing condition and biopolymer concentration, $DoBF_{final}$ exhibits a decreasing trend as porosity increases. For the 2.6% XG solution in the simple cubic packing condition, $DoBF_{final}$ declined from 20.3% at n = 0.3 to 16.2% (n = 0.35), 13.6% (n = 0.4), 12.7% (n = 0.5), and 9.1% (n = 0.6). Similarly, the 5.2% XG solution followed a comparable trend, with $DoBF_{final}$ values of 26.7%, 20.1%, 18.4%, 16.4%, and 10.9% at the respective porosity values. In contrast, the rhombohedral packing condition exhibited a more gradual reduction in $DoBF_{final}$, particularly in the lower porosity range ($0.3 \leq n \leq 0.4$). For the 2.6% XG solution, $DoBF_{final}$ decreased from 10.3% at n = 0.3 to 7.7% (n = 0.35), 6.2% (n = 0.4), 6.0% (n = 0.5), and 4.0% (n = 0.6). The 5.2% XG solution exhibited similar behavior, with $DoBF_{final}$ values of 12.7%, 11.6%, 11.1%, 11.0%, and 7.6%, respectively.

These findings indicate that different soil packing condition introduce upper and lower bounds for $DoBF_{final}$ at the same porosity. The simple cubic packing condition defines the upper bound, whereas the rhombohedral packing condition sets the lower bound. Notably, doubling the biopolymer concentration does not yield a proportional increase in $DoBF_{final}$, suggesting that a threshold concentration exists beyond which further biopolymer

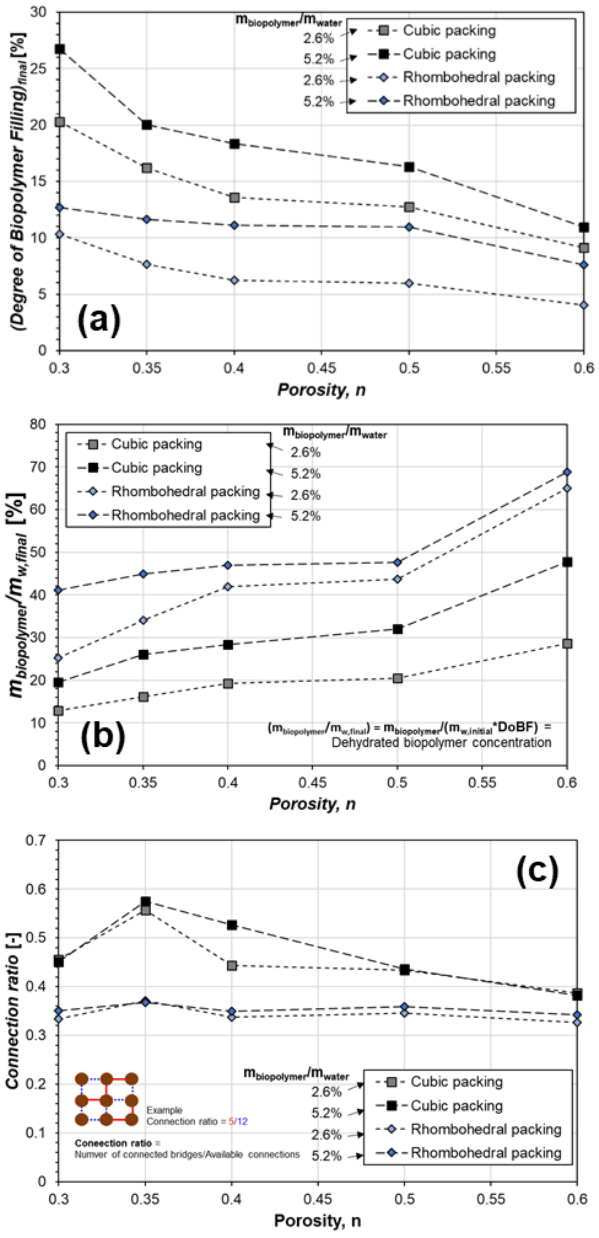

Fig. 8 Effect of porosity on biopolymer dehydration in terms of influencing factors

addition does not significantly improve soil stabilization. This observation highlights the importance of optimizing biopolymer input to maximize efficiency in practical applications.

Final Condensed Biopolymer Concentration and the Influence of Packing Structure

Assuming that the total injected biopolymer mass remains unchanged following water dehydration, the final mass of water retained within the soil matrix can be estimated. The final water mass is calculated from the two-dimensional monitored areas of *DoBF*. The final condensed biopolymer concentration is then derived using the equation:

$$\frac{m_{biopolymer}}{m_{w,final}} = \frac{m_{biopolymer}}{m_{initial\ water} \times DoBF}$$

For simple cubic packing condition, the 2.6% XG solution exhibited increasing final biopolymer concentrations as porosity increased, with values of 12.9% (n = 0.3), 16.2% (n = 0.35), 19.3% (n = 0.4), 20.5% (n = 0.5), and 28.6% (n = 0.6) (Fig. 8(b)). Notably, the expected final biopolymer concentration for the 5.2% XG solution did not reach twice that of the 2.6% solution due to the non-linear behavior of $DoBF_{final}$, reinforcing the concept of an optimal biopolymer concentration threshold. For example, while the 2.6% XG solution (under simple cubic packing) condensed to 12.9%, the 5.2% XG solution only reached 19.5%, which is significantly lower than twice the concentration of the 2.6% solution. A similar trend was observed for various porosity conditions, where the final biopolymer concentration of the 5.2% XG solution were recorded as 19.5% (n = 0.3), 26.1% (n = 0.35), 28.4% (n = 0.4), 32.0% (n = 0.5), and 47.8% (n = 0.6), at simple cubic packing condition.

The expected final biopolymer concentration was consistently higher in the rhombohedral soil packing condition than in the simple cubic soil packing condition. This phenomenon is attributed to the lower degree of biopolymer filling ($DoBF$) in rhombohedral packing, which allowed for a higher condensed biopolymer concentration. For instance, at n = 0.3, the $DoBF$ of the 2.6% XG solution in the simple cubic packing condition was 20.3%, whereas it was significantly lower at 10.3% in the rhombohedral packing condition. Consequently, the final biopolymer concentration was calculated as 12.9% for simple cubic packing and 25.2% for rhombohedral packing. Following this trend, the final biopolymer concentrations for the 2.6% XG solution in rhombohedral packing were estimated to be 25.2% (n = 0.3), 34.1% (n = 0.35), 41.9% (n = 0.4), 43.7% (n = 0.5), and 65.0% (n = 0.6). In contrast, for the 5.2% XG solution, the final biopolymer concentrations in rhombohedral packing were expected to be 41.1% (n = 0.3), 44.9% (n = 0.35), 47.0% (n = 0.4), 47.7% (n = 0.5), and 68.8% (n = 0.6).

Biopolymer Film Complexity and Its Contribution to Soil Strengthening

The complexity of the biopolymer film plays a crucial role in soil reinforcement, as the biopolymer matrix enhances tensile strength (Im 2020) and provides resistance to shear forces (Lee *et al.* 2019b). In this study, the complexity of the biopolymer film was assessed using the connection ratio, which quantifies the extent of interconnections within the biopolymer network. The connection ratio is defined as the fraction of actual connections relative to the total available connections within the porous matrix. The results indicate that the connection ratio reached its peak at n = 0.35, particularly in the simple cubic packing condition. This finding suggests that an optimal porosity exists for maximizing biopolymer film interconnectivity, thereby enhancing the overall mechanical stability of the soil matrix.

Table 2 The linear relationship between parameters from the microfluidic chip test and porosity

	m_b/m_s*	Soil packing condition	Relationship with parameter and porosity	
DoBF	1%	Simple cubic	$DoBF = 28.4 - 32.6\times(n)$	$(R^2 = 0.9)$
		Rhombohedral	$DoBF = 14.6 - 18.0\times(n)$	$(R^2 = 0.9)$
	2%	Simple cubic	$DoBF = 38.0 - 45.3\times(n)$	$(R^2 = 0.9)$
		Rhombohedral	$DoBF = 17.1 - 14.8\times(n)$	$(R^2 = 0.9)$
$(m_b/m_w)^*_{final}$	1%	Simple cubic	$(m_b/m_w)_{final} = 117.8\times(n) - 8.7$	$(R^2 = 0.9)$
		Rhombohedral	$(m_b/m_w)_{final} = 47.4\times(n) - 0.9$	$(R^2 = 0.9)$
	2%	Simple cubic	$(m_b/m_w)_{final} = 80.7\times(n) - 15.2$	$(R^2 = 0.8)$
		Rhombohedral	$(m_b/m_w)_{final} = 84.2\times(n) - 5.5$	$(R^2 = 0.9)$
connectivity	1%	Simple cubic	$connectivity = 0.6 - 0.4\times(n)$	$(R^2 = 0.5)$
		Rhombohedral	$connectivity = 0.4 - 0.1\times(n)$	$(R^2 = 0.1)$
	2%	Simple cubic	$connectivity = 0.7 - 0.4\times(n)$	$(R^2 = 0.4)$
		Rhombohedral	$connectivity = 0.37 - 0.04\times(n)$	$(R^2 = 0.2)$

* m_b/m_s: $m_{biopolymer}/m_{soil}$; m_b/m_w: $m_{biopolymer}/m_{water}$

For the 2.6% XG solution in the simple cubic soil packing condition, the connection ratios were measured as 0.46 (n = 0.3), 0.56 (n = 0.35), 0.44 (n = 0.4), 0.43 (n = 0.5), and 0.39 (n = 0.6). In contrast, the connection ratios in the rhombohedral packing condition were significantly lower, with values of 0.33 (n = 0.3), 0.37 (n = 0.35), 0.34 (n = 0.4), 0.35 (n = 0.5), and 0.33 (n = 0.6) (Fig. 8(c)).

Despite doubling the biopolymer concentration to 5.2%, the connection ratio did not increase proportionally. The experimental results demonstrated connection ratios of 0.45 (n = 0.3), 0.58 (n = 0.35), 0.53 (n = 0.4), 0.44 (n = 0.5), and 0.38 (n = 0.6) in the simple cubic soil packing condition. Moreover, the variation in connection ratio was relatively minimal for both the 5.2% XG solution and the rhombohedral packing condition, with values of 0.35 (n =0.3), 0.37 (n = 0.35), 0.35 (n = 0.4), 0.36 (n = 0.5), and 0.34 (n = 0.6).

Implications and Practical Considerations

The results suggest that a critical threshold exists in the effectiveness of biopolymer application for soil reinforcement. While an increase in biopolymer concentration leads to higher final biopolymer content, the effect is not strictly proportional due to water retention limitations and the physical constraints of the porous medium. Additionally, the connection ratio findings indicate that an optimal porosity level ($n \approx 0.35$) may exist where biopolymer network formation is maximized, enhancing soil stability.

Furthermore, the differences in soil packing conditions significantly affect both the degree of biopolymer filling and the final biopolymer concentration. Simple cubic packing facilitates a higher $DoBF$, leading to relatively lower final biopolymer concentrations. Conversely, rhombohedral packing, which exhibits lower $DoBF$, results in a more condensed biopolymer matrix (i.e., higher final biopolymer concentrations). These insights emphasize the importance of tailoring biopolymer injection strategies based on specific soil structural configurations to optimize reinforcement efficiency.

5. Discussion

A comprehensive analysis is conducted on the interrelationship between microscopic biofilm matrix formation and the macroscopic mechanical behavior of granular soils stabilized with XG hydrogel. Emphasis is placed on how porosity, degree of biopolymer filling ($DoBF$), condensed biopolymer concentration, and inter-particle connectivity influence the enhancement of soil strength.

The initial focus is on the correlation between these matrix parameters and unconfined compressive strength (UCS), identifying porosity as the most dominant factor governing strength performance. Through data interpolation and curve fitting techniques, a unified predictive model is developed that integrates previously reported UCS values with experimental findings.

Subsequent analysis explores the effect of XG treatment on shear strength parameters—cohesion and internal friction angle—across different biopolymer concentrations and soil packing structures. The contrast between simple cubic and rhombohedral packing conditions provides insights into the boundaries of biopolymer-based soil treatment (BPST).

To validate these correlations, back-calculation techniques are applied to estimate UCS and shear strength from known porosity. The results contribute to a mechanistic understanding of biopolymer-soil interaction and offer a basis for optimized design in bio-mediated ground improvement.

5.1 Correlation of biofilm matrix formation with soil strengthening parameters

The reinforcement performance of XG in soils has been

Table 3 The linear relationship between unconfined compressive strength, porosity and the parameters from this study

	Soil packing condition	*UCS*	
DoBF	Simple cubic	$UCS = 6332 - 6655\times(n) - 8.292\times(DoBF)$	$(R^2 = 0.56)$
	Rhombohedral	$UCS = 6295 - 6620\times(n) - 13.79\times(DoBF)$	$(R^2 = 0.56)$
$(m_b/m_w)_{final}$	Simple cubic	$UCS = 6069 - 5391\times(n) - 10.14\times(m_b/m_w)_{final}$	$(R^2 = 0.57)$
	Rhombohedral	$UCS = 6109 - 5298\times(n) - 26.47\times(m_b/m_w)_{final}$	$(R^2 = 0.58)$
connectivity	Simple cubic	$UCS = 6645 - 6752\times(n) - 927.9\times(connectivity)$	$(R^2 = 0.57)$
	Rhombohedral	$UCS = 6580 - 6469\times(n) - 1421\times(connectivity)$	$(R^2 = 0.58)$

Table 4 The linear relationship between unconfined compressive strength, porosity and the parameters from this study

	Soil packing condition	*Cohesion (c)*	
DoBF	Simple cubic	$c = 23.56\times(DoBF) + 55.84\times(n) + 176.4$	$(R^2 = 0.35)$
	Rhombohedral	$c = 44.99\times(DoBF) + 124.4\times(n) - 192.5$	$(R^2 = 0.42)$
$(m_b/m_w)_{final}$	Simple cubic	$c = 583.7 - 1855\times(n) + 9.708\times(m_b/m_w)_{final}$	$(R^2 = 0.35)$
	Rhombohedral	$c = 498.9 - 1593\times(n) + 18.07\times(m_b/m_w)_{final}$	$(R^2 = 0.43)$
connectivity	Simple cubic	$c = 241.4 - 865.4\times(n) + 705.1\times(connectivity)$	$(R^2 = 0.21)$
	Rhombohedral	$c = 313.4 - 1037\times(n) + 951.6\times(connectivity)$	$(R^2 = 0.21)$
		Friction angle (ϕ)	
DoBF	Simple cubic	$\phi = 210 - 483.3\times(n) + 0.5751\times(DoBF)$	$(R^2 = 0.76)$
	Rhombohedral	$\phi = 211.6 - 485.2\times(n) + 1.012\times(DoBF)$	$(R^2 = 0.77)$
$(m_b/m_w)_{final}$	Simple cubic	$\phi = 228.4 - 530\times(n) + 0.2415\times(m_b/m_w)_{final}$	$(R^2 = 0.76)$
	Rhombohedral	$\phi = 227.3 - 523.9\times(n) + 0.4009\times(m_b/m_w)_{final}$	$(R^2 = 0.77)$
connectivity	Simple cubic	$\phi = 217.6 - 502.2\times(n) + 20.09\times(connectivity)$	$(R^2 = 0.75)$
	Rhombohedral	$\phi = 218.5 - 505.8\times(n) + 28.94\times(connectivity)$	$(R^2 = 0.76)$

primarily evaluated through unconfined compressive strength (*UCS*) measurements. In previous studies, the *UCS* of XG-treated Korean residual soil (CH) reached up to 6.0 MPa with a 1% XG treatment (Chang *et al*. 2015b). Similarly, *UCS* values varied depending on soil type, with 880 kPa reported for treated sand (SP), 4,940 kPa for red-yellow soil (CL), and up to 6,240 kPa for high-plasticity clay (CH) treated with 1% XG (Kwon *et al*. 2019). In the case of silty sand (SM) treated with 2% XG, the *UCS* was recorded at 4,880 kPa (Lee *et al*. 2019a). Due to differences in relative density across test specimens, the *UCS* values from these studies were reanalyzed in terms of soil porosity to enable consistent comparison.

The derived relationship can be expressed as $UCS = -5800.6 \times (n) + 5901.3$, where *UCS* denotes the uniaxial compressive strength (kPa), and n represents the porosity. The equation reflects a decreasing trend in *UCS* with increasing porosity, consistent with the findings reported in previous study using cemented soil (Wei and Ku 2020b).

The interrelationship between *UCS*, porosity, and key parameters such as *DoBF*, condensed biopolymer concentration, and connectivity, which derived from the laboratory experiments was analyzed. Linear correlations between these parameters and porosity were interpolated, as summarized in Table 2. In addition to data corresponding to 1.0% and 2.0% $m_{biopolymer}/m_{soil}$, interpolations were extended to include intermediate concentrations of 0.5% and 1.5%.

Subsequently, *UCS* values reported in previous studies were also interpolated linearly, as summarized in Table 3 ($R^2 \approx 0.6$). A simple polynomial curve fitting method was employed using the Curve Fitting Toolbox in MATLAB (The MathWorks, Inc., Version R2022a). Among all the evaluated parameters, porosity exhibited the most dominant influence on *UCS*, regardless of the specific biopolymer matrix formation parameter. This strong inverse relationship between porosity and *UCS* was consistently observed throughout the analysis.

Correlation with shear parameters

The untreated soil exhibited an increase in deviatoric strength from 412 kPa to 893 kPa as the confining pressure (σ_3) increased from 100 kPa to 200 kPa. Although the Mohr–Coulomb analysis yielded a cohesion value of 18.3 kPa and a friction angle of 41°, the cohesion was considered negligible due to the cohesionless nature of the tested sand.

Upon biopolymer treatment and sufficient drying time, the development of the biopolymer film matrix led to a significant increase in deviatoric stress. With 0.5% biopolymer content ($m_{biopolymer}/m_{soil}$), deviatoric stress increased to 1208 kPa (σ_3 = 50 kPa), 1367 kPa (σ_3 = 100

Table 5 Expectation of unconfined compressive strength and cohesion using the expected correlationship

Parameter	Biopolymer content [%]	Soil packing condition	Expected *UCS* [kPa]	Expect error* [%]
DoBF [%]	1%	Simple cubic	3031.9	2.7
		Rhombohedral	3035.2	2.6
	2%	Simple cubic	2965.8	4.9
		Rhombohedral	2979.6	4.4
$(m_b/m_w)_{final}$ [%]	1%	Simple cubic	2996.2	3.9
		Rhombohedral	2987.5	4.2
	2%	Simple cubic	3242.7	4.0
		Rhombohedral	2641.7	15.2
connectivity	1%	Simple cubic	3025.5	2.9
		Rhombohedral	2974.7	4.6
	2%	Simple cubic	2932.7	5.9
		Rhombohedral	2976.4	4.5
Parameter	Biopolymer content [%]	Soil packing condition	Expected *c* [kPa]	Expect error* [%]
DoBF [%]	1%	Simple cubic	150.8	6.1
		Rhombohedral	135.4	15.7
	2%	Simple cubic	233.3	24.3
		Rhombohedral	316.9	68.8
$(m_b/m_w)_{final}$ [%]	1%	Simple cubic	157.8	1.7
		Rhombohedral	129.1	19.6
	2%	Simple cubic	78.2	58.3
		Rhombohedral	365.2	94.6
connectivity	1%	Simple cubic	113.7	29.2
		Rhombohedral	150.6	6.2
	2%	Simple cubic	184.2	1.9
		Rhombohedral	149.5	20.4

*Expect error = $(E - M)/M$, where E is the expected value and M is the measured (real) value

kPa), and 1656 kPa (σ_3 = 200 kPa). At 1.0% biopolymer content, higher deviatoric strengths were observed: 1475 kPa, 2026 kPa, and 2543 kPa at corresponding confining pressures. When the biopolymer content was increased to 2.0%, deviatoric stresses reached 3243 kPa, 3310 kPa, and 3767 kPa, respectively. Mohr–Coulomb analysis was used to calculate shear strength parameters. Cohesion values were determined as 160.6 kPa, 187.7 kPa, and 218.4 kPa for the 0.5%, 1.0%, and 2.0% biopolymer contents, respectively. Corresponding friction angles were 32.1°, 34.6°, and 38.4°, demonstrating that both cohesion and internal friction improved with increasing biopolymer dosage.

The interrelationship was analyzed using a three-dimensional interpolation method, as outlined in Table 4, based on the assessed shear strength parameters—namely, cohesion (c) ($R^2 \approx 0.4$) and friction angle (ϕ) ($R^2 \approx 0.8$). Two distinct correlation patterns were identified for simple cubic and rhombohedral soil packing conditions, representing the lower and upper bounds, respectively, for shear strength behavior across varying porosities. The results indicate that rhombohedral packing conditions define the upper bound for expected cohesion values within the practical porosity range of 0.2–0.7. This is supported by a previous study which identified a porosity range of 0.26–0.48 for rhombohedral and simple cubic packing in uniform spherical grain assemblies (Artiola *et al.* 2004). Conversely, the simple cubic packing condition was associated with the lower bound of cohesion expectation, highlighting the influence of soil structure on biopolymer-induced shear strength development.

5.2 Back-calculation using the correlated relationship

Previous studies have reported a typical porosity of 0.48 for biopolymer-treated soils. Using the established correlation between porosity and uniaxial compressive strength (*UCS*) presented in Section 5.1, the *UCS* at this porosity was estimated to be 3117.0 kPa, which is assumed here as the reference (measured) value. Based on this porosity, biopolymer matrix formation parameters—namely, the degree of biopolymer filling (*DoBF*), final condensed biopolymer concentration, and connectivity—were predicted using the empirical relationships presented in Table 2. Subsequently, the *UCS* was calculated through the interpolation model summarized in Table 3, and the predicted results are provided in Table 5.

Among the three parameters, *DoBF* yielded the most accurate *UCS* predictions, showing the smallest deviation from the reference value. In most cases, the relative error in *UCS* prediction was less than 10%, except for the case involving the condensed biopolymer concentration at a 2%

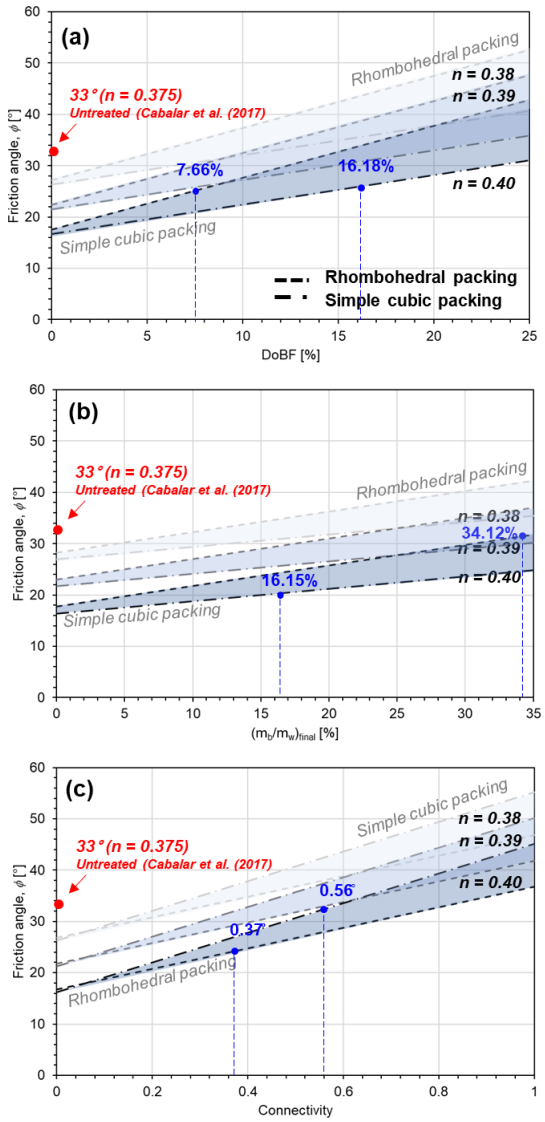

Fig. 9 Expectation of friction angle with the parameters related to biopolymer film matrix formation

biopolymer-to-soil treatment ratio under rhombohedral packing conditions.

Cohesion values were determined to be 160.6 kPa for 1% biopolymer treatment and 187.7 kPa for 2% treatment. Compared to *UCS* predictions, the expected cohesion values exhibited larger relative errors. However, interpolation results (Table 5) showed improved accuracy for the 1% treatment case compared to the 2%, with relative errors generally below 20%—except connenctivity underthe 1% treatment condition with simple cubic packing condition.

To compare with the friction angle reported in previous studies, the estimation was conducted within a porosity range of 0.38 to 0.40. According to Cabalar et al. (2017), the friction angle for untreated soil was assessed as 33° at a porosity of 0.375. In this study, the formation of the biopolymer film matrix was observed to vary depending on the soil packing condition, as illustrated in Fig. 5. The effects of matrix formation parameters—namely the degree of biopolymer filling (*DoBF*), condensed biopolymer concentration, and connectivity—at n = 0.4 and nearby porosity values were incorporated into the friction angle prediction curves presented in Fig. 9 Three biopolymer matrix formation parameters obtained from the laboratory experimental program—*DoBF*, condensed biopolymer concentration, and connectivity—were plotted to estimate the friction angle. The results indicate that *DoBF* provides the narrowest range of friction angle predictions at a given porosity. For instance, at n = 0.4, a *DoBF* of 7.66% under rhombohedral packing condition corresponded to a friction angle of 25.27°, whereas a higher *DoBF* of 16.18% resulted in a slightly increased friction angle of 25.98°. These findings suggest that *DoBF* is sensitive to XG dehydration conditions, and the friction angle of XG-treated soil at n = 0.4 can reasonably be expected to fall within the range of 25.27° to 25.98°.

Application Potential and Density-Based Optimization Strategy

In recent years, the demand for sustainable and environmentally friendly soil improvement methods has led to the growing use of biopolymers such as XG in geotechnical engineering. XG, a naturally derived polysaccharide, has been shown to effectively enhance soil strength through the formation of a cohesive biopolymer matrix, offering a promising alternative to traditional chemical stabilizers like cement or lime.

This material has already demonstrated its effectiveness in various geotechnical applications. For instance, it has been used in embankment stabilization for infrastructure projects, where a small addition of XG—typically around 1% of the total soil weight-can significantly increase mechanical stability while maintaining low environmental impact (Kwon *et al.* 2023b). Additionally, slope protection and erosion control have benefited from XG-treated soils, as the biopolymer improves cohesion and reduces surface runoff effects. In dispersive or collapsible soils, XG also reduces soil erodibility and increases resistance to particle detachment, thereby minimizing long-term deformation risks

In light of these applications, this study highlights the importance of targeting a specific soil density during field implementation. The mechanical behavior of biopolymer-treated soils, particularly in terms of strength and film connectivity, is highly influenced by porosity, which is inversely related to soil density. Our results indicate that, rather than relying solely on increasing biopolymer content, it is more efficient—both economically and technically—to achieve an optimal target density that promotes uniform biopolymer distribution and effective matrix formation. By doing so, practitioners can maximize the mechanical performance of treated soils while minimizing unnecessary material usage, leading to more sustainable and cost-effective soil improvement solutions.

6. Conclusions

This study demonstrated that biopolymer-based soil treatment (BPST) enhances mechanical performance through the formation of biopolymer matrix networks

within soil voids. By experimentally evaluating the effects of biopolymer concentration, porosity, and soil packing conditions, key parameters such as the degree of biopolymer filling (*DoBF*), final condensed biopolymer concentration, and connectivity were quantified. The findings revealed that while higher biopolymer concentrations increase the final biopolymer volume, the relationship is non-linear due to threshold effects. Rhombohedral packing yielded higher condensed biopolymer concentrations compared to simple cubic packing, despite having lower *DoBF* values. Furthermore, optimal biopolymer connectivity was observed at a porosity of approximately 0.35.

Correlations between biopolymer matrix formation and mechanical properties—namely uniaxial compressive strength (*UCS*), cohesion, and friction angle—were established. *UCS* showed a negative correlation with porosity, and predictive models confirmed that *DoBF* most accurately estimates both *UCS* and friction angle. Rhombohedral and simple cubic packings respectively represented the upper and lower bounds for cohesion expectations.

These results underscore the importance of density-controlled design in biopolymer-treated soils. Adjusting porosity and biopolymer input allows for targeted optimization of soil strength. The study provides a foundation for developing practical and sustainable biopolymer injection strategies in geotechnical engineering, ensuring improved mechanical performance and efficient material use.

Acknowledgments

This work was supported by the National Research Foundation of Korea (NRF) grant funded by the Korea government (MSIT) (No.2022R1A2C2091517).

References

Acharya, R., Pedarla, A., Bheemasetti, T.V. and Puppala, A.J. (2017), "Assessment of guar gum biopolymer treatment toward mitigation of desiccation cracking on slopes built with expansive soils", *Transport. Res. Record*, **2657**(1), 78-88. https://doi.org/10.3141/2657-0.

Aparna, R.P. and Bindu, J. (2023), "Utilization of waste material as a substitute for the sand drain in clayey soil", *Int. J. Geo-Eng.*, **14**(1), 2. http://doi.org/10.1186/s40703-022-00180-9.

Artiola, J.F., Pepper, I.L. and Brusseau, M.L. (2004*), Environmental monitoring and characterization (Eds.),* Academic Press.

Ayeldeen, M.K., Negm, A.M. and El Sawwaf, M.A. (2016), "Evaluating the physical characteristics of biopolymer/soil mixtures", *Arab. J. Geosci.*, **9**, 1-13. http://doi.org/10.1007/s12517-016-2366-1.

Barcelo, L., Kline, J., Walenta, G. and Gartner, E. (2014), "Cement and carbon emissions", *Mater. Struct.*, **47**(6), 1055-1065. http://doi.org/s11527-013-0114-5.

Cabalar, A.F., Wiszniewski, M. and Skutnik, Z. (2017), "Effects of xanthan gum biopolymer on the permeability, odometer, unconfined compressive and triaxial shear behavior of a sand", *Soil Mech. Found. Eng.*, **54**(5), 356-361. http://doi.org/10.1007/s11204-017-9481-1.

Chang, I., Im, J., Prasidhi, A.K. and Cho, G.C. (2015a), "Effects of xanthan gum biopolymer on soil strengthening", *Constr. Build. Mater.*, **74**, 65-72. https://doi.org/10.1016/j.conbuildmat.2014.10.026.

Chang, I., Jeon, M. and Cho, G.C. (2015b), "Application of microbial biopolymers as an alternative construction binder for earth buildings in underdeveloped countries", *Int. J. Polymer Sci.*, **2015**, 326745. https://doi.org/10.1155/2015/326745.

Chang, I., Im, J. and Cho, G.C. (2016), "Introduction of microbial biopolymers in soil treatment for future environmentally-friendly and sustainable geotechnical engineering", *Sustainability*, **8**(3), 251. http://doi.org/10.3390/su8030251.

Chang, I., Kwon, Y.M., Im, J. and Cho, G.C. (2019), "Soil consistency and interparticle characteristics of xanthan gum biopolymer–containing soils with pore-fluid variation", *Can. Geotech. J.*, **56**(8), 1206-1213. https://doi.org/10.1139/cgj-2018-0254.

Chu, J., Varaksin, S., Klotz, U. and Mengé, P. (2009), "Construction Processes: State-of-the-art Report", *Proceedings of the 17th International Conference on Soil Mechanics and Geotechnical Engineering*, Alexandria, Egypt, September.

Eslami, A., Moshfeghi, S., Molaabasi, H. and Eslami, M.M. (2019), *Piezocone and Cone Penetration test (CPTu and CPT) Applications in Foundation Engineering*, Butterworth-Heinemann, Oxford, United Kingdom. http://doi.org/10.1016/C2017-0-04195-2.

Fatehi, H., Ong, D.E., Yu, J. and Chang, I. (2021), "Biopolymers as green binders for soil improvement in geotechnical applications: a review", *Geosci.*, **11**(7), 291. https://doi.org/10.3390/geosciences11070291.

García-Ochoa, F., Santos, V., Casas, J. and Gomez, E. (2000), "Xanthan gum: production, recovery, and properties", *Biotech. Adv.*, **18**(7), 549-579. https://doi.org/10.1016/S0734-9750(00)00050-1.

Ham, S.M., Chang, I., Noh, D.H., Kwon, T.H. and Muhunthan, B. (2018), "Improvement of surface erosion resistance of sand by microbial biopolymer formation", *J. Geotech. Geoenviron. Eng.*, **144**(7), 06018004. https://doi.org/10.1061/(ASCE)GT.1943-5606.0001900.

Hataf, N., Ghadir, P. and Ranjbar, N. (2018), "Investigation of soil stabilization using chitosan biopolymer", *J. Cleaner Product.*, **170**, 1493-1500. https://doi.org/10.1016/j.jclepro.2017.09.256.

Im, J. (2020), "Polysaccharide Biopolymers in Sands: Properties and Behaviors", Ph.D. Dissertation; Korea Advanced Institute of Science and Technology (KAIST), Daejeon, South Korea.

Katzbauer, B. (1998), "Properties and applications of xanthan gum", *Polymer Degradat. Stab.*, **59**(1-3), 81-84. https://doi.org/10.1016/S0141-3910(97)00180-8.

Kwon, Y.M., Chang, I., Lee, M. and Cho, G.C. (2019), "Geotechnical engineering behaviors of biopolymer-treated soft marine soil", *Geomech. Eng.*, **17**(5), 453-464. http://doi.org/10.12989/gae.2019.17.5.453.

Kwon, Y.M., Ham, S.M., Kwon, T.H., Cho, G.C. and Chang, I. (2020), "Surface-erosion behaviour of biopolymer-treated soils assessed by EFA", *Géotechnique Lett.*, **10**(2), 1-7. https://doi.org/10.1680/jgele.19.00106.

Kwon, Y.M., Kang, S.J., Cho, G. C. and Chang, I. (2023a), "Effect of microbial biopolymers on the sedimentation behavior of kaolinite", *Geomech Eng*, **33**, 121-131. http://doi.org/10.12989/gae.2023.33.2.121.

Kwon, Y. M., Moon, J. H., Cho, G.C., Kim, Y.U. and Chang, I. (2023b), "Xanthan gum biopolymer-based soil treatment as a construction material to mitigate internal erosion of earthen embankment: A field-scale", *Constr. Build. Mater.*, **389**, 131716. http://doi.org/10.1016/j.conbuildmat.2023.131716.

Latifi, N., Horpibulsuk, S., Meehan, C.L., Majid, M.Z.A. and

Rashid, A.S.A. (2016), "Xanthan gum biopolymer: an eco-friendly additive for stabilization of tropical organic peat", *Environ. Earth Sci.*, **75**, 1-10. http://doi.org/10.1007/s12665-016-5643-0.

Lee, S., Chung, M., Park, H.M., Song, K.I. and Chang, I. (2019a), "Xanthan gum biopolymer as soil-stabilization binder for road construction using local soil in Sri Lanka", *J. Mater. Civil Eng.*, **31**(11), 06019012.

Lee, S., Im, J., Cho, G.C. and Chang, I. (2019b), "Laboratory triaxial test behavior of xanthan gum biopolymer-treated sands", *Geomech. Eng.*, **17**(5), 445-452. https://doi.org/10.12989/gae.2019.17.5.445.

Lee, M., Chang, I., Kang, S.J., Lee, D.H. and Cho, G.C. (2023), "Alkaline induced-cation crosslinking biopolymer soil treatment and field implementation for slope surface protection", *Geomech. Eng.*, **33**(1), 29-40. https://doi.org/10.12989/gae.2023.33.1.029.

Makusa, G.P. (2013), "Soil stabilization methods and materials in engineering practice: State of the art review", Lulea tekniska universitet.

Orts, W., Roa-Espinosa, A., Sojka, R., Glenn, G., Imam, S., Erlacher, K. and Pedersen, J. (2007), "Use of synthetic polymers and biopolymers for soil stabilization in agricultural, construction, and military applications", *J. Mater. Civil Eng.*, **19**(1), 58-66. https://doi.org/10.1061/(ASCE)0899-1561(2007)19:1(58).

Saxena, S., Roy, L.B., Gupta, P.K., Kumar, V. and Paramasivan, P. (2024), "Model tests on ordinary and geosynthetic encased stone columns with recycled aggregates as filler material", *Int. J. Geo-Eng.*, **15**(1), 1. http://doi.org/10.1186/s40703-023-00202-0.

Schaefer, V.R., Mitchell, J.K., Berg, R.R., Filz, G.M. and Douglas, S.C. (2012), "Ground Improvement in the 21st Century: A Comprehensive Web-based Information System", *Geotechnical Engineering State of the Art and Practice: Keynote Lectures from GeoCongress 2012*, Oakland, California, March.

Shalchian, M.M., Arabani, M., Farshi, M. and Ranjbar, P.Z. (2025), "Sustainable construction materials: Application of chitosan biopolymer, rice husk biochar, and hemp fibers in geo-construction", *Case Stud. Constr. Mater.*, **22**, e04528. http://doi.org/10.1016/j.cscm.2025.e04528.

Tran, A.T.P., Chang, I. and Cho, G.C. (2019), "Soil water retention and vegetation survivabiity improvement using microbial biopolymers in drylands", *Geomech. Eng.*, **17**(5), 475-483. http://doi.org/10.12989/gae.2019.17.5.475.

Wei, J. and Ku, T. (2020a), "Strength behavior of cemented sand considering the influence of porosity and curing conditions", *Constr. Build. Mater.*, **234**, 117385. https://doi.org/10.1016/j.conbuildmat.2019.117385.

Wei, X. and Ku, T. (2020b), "New design chart for geotechnical ground improvement: characterizing cement-stabilized sand", *Acta Geotechnica*, **15**, 999-1011. http://doi.org/10.1007/s11440-019-00838-2.

Williams, P.A. and Phillips, G.O. (Eds.). (2000*), Gums and stabilisers for the food industry* **10**. Woodhead publishing.

Zulfikar, R. A., Yasuhara, H., Kinoshita, N. and Putra, H. (2022), "Utilization of carrageenan as an alternative eco-biopolymer for improving the strength of liquefiable soil", *Proceedings of the 2022 World Congress on Advances in Civil, Environmental, and Materials Research (ACEM22)*, Seoul, August.